Journal of Theoretical and Applied Information Technology
31st October 2026. Vol.104. No.20
© Little Lion Scientific
ISSN: 1992-8645 www.jatit.org E-ISSN: 1817-3195

TEMPORAL TAG–GUIDED MULTI-TASK GENERATIVE TRANSFORMER FOR HORIZON-AWARE TWEET-DRIVEN STOCK DIRECTION FORECASTING

S. PUNITHA[1], G.K. ARUN[2]

[1]Research Scholar, PG & Research Department of Computer Science, Aringar Anna Governemnt Arts College, Villupuram, Tamilnadu, India

[2]Assistant Professor, PG & Research Department of Computer Science, Aringar Anna Governemnt Arts College, Villupuram, Tamilnadu, India

E-mail: [1]punithaphd2024@gmail.com, [2]arunnura2370@gmail.com

ABSTRACT

Understanding the influence of social sentiment on stock market behavior has become essential in financial forecasting. Tweets, rich in emotion and immediacy, often reflect public reactions to market events before traditional indicators respond. This work introduces a temporal tag–guided, multi-task text generation framework that interprets tweet sentiment for stock movement prediction. By embedding financial time context directly into each input, the model learns to align language with specific market phases. The architecture simultaneously decodes sentiment classification, short- and long-term price direction, and event-driven rationale in a structured output format. A text-to-text transformer approach ensures adaptability across tasks without requiring separate models. The integration of temporal understanding with unified decoding enables more accurate, interpretable, and horizon-aware forecasts from unstructured tweet streams. This design bridges the gap between informal emotional language and structured financial logic, supporting intelligent systems that respond to the rhythm of market sentiment in real time.

Keywords: *Financial Sentiment Analysis - Tweet-Based Stock Prediction - Temporal Tagging - Multi-Task Text Generation - Text-to-Text Transformer - Horizon-Aware Market Forecasting*

1. INTRODUCTION

Sentiment analysis has evolved into a crucial analytical process that deciphers the underlying emotion, opinion, or attitude within text-based content. Public expression through digital platforms has made social text, particularly microblogging data, a powerful signal for measuring collective psychological trends [1]. Among these platforms, Twitter holds a distinctive position. With its high-frequency, real-time stream of diverse user opinions, Twitter provides immediate and wide-reaching reflections of public mood. This massive flow of unfiltered and unmoderated social commentary generates patterns that often parallel real-world reactions. Tweets have come to represent more than mere social chatter they offer observable fluctuations in emotional states that resonate across sectors, including politics, health, and financial systems [2].

Within contemporary society, Twitter's influence has permeated sensitive domains such as financial markets. Stock trading behavior, once shaped primarily by expert analysis and economic reports, now shows sensitivity to online sentiment waves. Public expressions of trust, fear, or optimism about a company or the economy can ripple through trading patterns within minutes [3]. Market psychology, amplified through viral hashtags or influential user commentary, reveals how collective emotion triggers tangible effects on asset movements. When tweets referencing financial news, corporate actions, or macroeconomic events begin to trend, investor communities react with noticeable shifts in trading volume and volatility. This feedback loop between social dialogue and trading actions underscores a new paradigm in market behavior, where tweets function as both indicators and catalysts [4].

Stock market prediction, particularly under short-horizon or volatile conditions, increasingly demands attention to non-traditional data sources. Tweets, when mapped against price fluctuations

and event outcomes, offer early clues to crowd sentiment. Extracting meaningful indicators from tweet streams requires the ability to navigate informal language, sarcasm, hashtags, abbreviations, and emotionally loaded expressions [5]. Traditional financial indicators often lag behind these sentiment cues. This gap has motivated the incorporation of machine learning and deep learning models that specialize in processing unstructured language data. These models not only detect sentiment but can infer its potential directional impact on financial instruments [6].

Deep learning offers structural advantages in handling the complexity of tweet-based forecasting. With its capacity for non-linear transformation, deep networks can model subtleties within sentiment variation, temporal sequences, and context shifts. Language models built on recurrent or transformer architectures outperform rule-based systems in interpreting emotional language, trend signals, and market associations[7]. Neural embeddings can capture the context of terms based on co-occurrence and sentence position, enabling finer sentiment discrimination. When applied to the financial domain, these models allow prediction systems to process raw tweet text and generate insights aligned with trading logic. The convergence of sentiment signals and price trajectory modeling supports enhanced predictive capability, especially under market stress or information shocks [8].

The emergence of generative transformer models, particularly those designed under the text-to-text formulation, has further expanded the scope of tweet-based financial prediction. Text-to-Text Transfer Transformer (T5) presents a unified architecture that interprets every task classification, extraction, summarization as a translation from one text format to another [9]. This format enables multitask learning with a shared model backbone, facilitating simultaneous processing of sentiment classification, market trend direction, and event explanation. The structure accommodates both emotional and temporal signals, ensuring more accurate alignment between tweet content and financial movement [10]. Temporal prompt engineering extends this architecture by embedding time-specific cues directly into the input text. Each tweet, when tagged with a contextual time label such as “pre-market volatility” or “post-earnings dip,” provides the model with insight into the financial conditions under which the sentiment was expressed. This embedding allows the model to consider not just what was said, but when it was said, anchoring sentiment in the correct market context. Multi-task learning, layered onto this temporal foundation, enables concurrent generation of sentiment labels, price direction forecasts, and market-relevant explanations. This integration of temporal conditioning and multi-output modeling within the T5 structure opens new frontiers for predictive analytics grounded in financial social signals.

The study is structured to ensure direct correspondence between conceptual objectives and empirical validation. The objective of integrating temporal market conditioning with unified multi-task decoding is evaluated through quantitative metrics that measure classification correctness, correlation robustness, detection reliability, and precision–recall balance. Each architectural component introduced in the methodology is reflected in measurable performance indicators reported in the Results section. This alignment guarantees that the proposed temporal tagging strategy, structured generative output design, and horizon-aware forecasting mechanism are not only conceptual contributions but empirically validated advancements within tweet-driven financial prediction.

1.1. Problem Statement

Stock market movements are increasingly influenced by real-time public sentiment expressed through social media, particularly tweets. Traditional predictive models often fail to account for the linguistic ambiguity, emotional intensity, and temporal variability inherent in these social signals. Static classifiers and delayed indicators miss short-horizon sentiment shifts and market-relevant cues embedded in informal language. The absence of temporally conditioned, multi-task capable frameworks leads to incomplete analysis of tweet-driven stock behavior. Current models lack the structural capacity to simultaneously interpret sentiment, forecast price direction, and contextualize financial events from a single textual input. A unified model that integrates temporal understanding and multi-field decoding remains critically underexplored in financial sentiment prediction.

1.2. Motivation and objective

Rapid growth of social media discourse has reshaped stock market dynamics, with tweets acting as early indicators of investor emotion, risk perception, market expectation. Conventional

prediction systems struggle to capture informal language, emotional volatility, temporal sensitivity present in tweet streams. This gap motivates development of a unified framework capable of decoding sentiment signals, market direction, contextual rationale within a single analytical flow. The objective focuses on designing a temporal tag–guided, multi-task generative architecture built upon the T5 text-to-text paradigm. The framework aims to integrate temporal awareness, sentiment interpretation, horizon-aware trend forecasting, structured explanation generation. Such integration seeks to enhance contextual accuracy, interpretability, scalability of tweet-driven stock market prediction under rapidly changing financial conditions.

1.3. Research Design

This study addresses the challenge of temporally misaligned sentiment interpretation in tweet-driven stock forecasting. Existing frameworks either classify sentiment without market anchoring or predict price direction without structured linguistic conditioning. The research design follows a temporally synchronized, multi-task generative architecture. Tweet streams are aligned with real-time market signals through volatility-aware tagging. A structured text-to-text transformer model is trained to simultaneously generate sentiment polarity, short-term and long-term directional forecasts, and contextual event rationale within a unified decoding pipeline. Experimental validation employs supervised training over a temporally segmented financial tweet dataset, followed by comparative evaluation against established sentiment models using classification and correlation-based metrics. This design ensures methodological coherence between temporal conditioning, multi-field decoding, and empirical benchmarking.

2. LITERATURE REVIEW

"Hybrid Conflict Lens" [11] composite deep learning workflow integrating multi-filter convolution layers with bidirectional long short-term memory units for contextual polarity capture. Tweet streams underwent normalization, token encoding, sentiment labeling through supervised learning, followed by latent semantic extraction via probabilistic topic modeling. Feature fusion supported sequential dependency learning across conflict narratives. Optimization relied on gradient-based tuning with balanced class handling. "Optimized Linguistic Mapper" [12] applied linguistics-driven preprocessing with deep neural sentiment classifiers enhanced through sine cosine optimization. Lexical normalization, syntactic pruning, semantic polarity tagging formed the linguistic foundation. Neural parameters underwent iterative tuning using oscillatory optimization to escape local minima. Fitness evaluation relied on convergence stability rather than outcome dominance. "Emotion Signal Miner" [13] employed large-scale tweet crawling integrated with emotion lexicons mapped onto sentiment polarity dimensions. Textual streams passed through noise filtering, emotional token extraction, multi-class labeling aligned with mental health indicators. Statistical normalization connected micro-level emotional signals with macro-level public health statistics. Machine learning classifiers learned emotional intensity distributions without dependence on demographic identifiers.

"Bias Audit Framework" [14] introduced a structured audit pipeline evaluating sentiment label disparities across domains. Foundation models generated polarity annotations over heterogeneous datasets spanning reviews plus microblogs. Parallel human annotations served as reference benchmarks. Statistical bias metrics quantified divergence patterns across demographic-neutral categories. "Athlete Sentiment Transfer" [15] using pretrained language encoders fine-tuned on sports-centric tweet corpora. Domain adaptation focused on negative sentiment cues expressed through fan discourse. Layer freezing strategies preserved semantic priors while task-specific heads captured hostility markers. Data augmentation addressed class imbalance through controlled sampling. "Financial Polarity Engine" [16] employed classical machine learning classifiers supported by finance-aware feature engineering. Token filtering removed noise terms unrelated to market semantics. Sentiment lexicons enriched with financial indicators guided feature vector construction. Supervised learning trained polarity predictors under strict temporal alignment.

"Cyber Harm Analyzer" [17] combined sentiment polarity detection with aggression cue extraction to flag cyberbullying content. Text streams passed through toxicity filters, emotional intensity scoring, contextual threat identification. Machine learning classifiers learned abusive patterns without identity inference. Psychological impact assessment relied on aggregated sentiment

severity indices. "Fashion Mood Hybrid" [18] implemented a hybrid architecture merging transformer-based contextual encoders with recurrent neural units. Fashion-related tweets underwent semantic embedding through attention mechanisms followed by temporal refinement. The sequential layer captured stylistic sentiment evolution across posts. Training emphasized representation balance between trend descriptors, emotional adjectives. "Aspect Segmentation Engine" [19] integrated aspect-level sentiment parsing with unsupervised text mining for customer clustering. Social content underwent aspect extraction, polarity scoring per product attribute, vector aggregation. Clustering algorithms grouped users based on sentiment-aspect profiles. "Graph Political Encoder" [20] adopted a graph-enhanced pretrained language model embedding relational structures among users, topics, sentiments. Social interactions formed graph edges enriching textual embeddings. Pretraining incorporated syntactic patterns from Filipino language constructs. Fine-tuning targeted political discourse polarity classification. "Semantic Tweet Synthesizer" [21] combined semantic feature extraction with intelligent clustering preceding supervised classification. Tweets underwent embedding generation, similarity-based grouping, noise isolation. Cluster-aware classifiers learned sentiment patterns within homogeneous semantic regions. "Election Language Adapter" [22] a domain-specific BERT variant pretrained on election discourse. Tokenization incorporated political entities, campaign terminology. Contextual embeddings fed classification heads tailored for polarized conversations. Training emphasized temporal coherence across election cycles. The approach highlighted domain-adaptive pretraining, linguistic nuance capture, scalable deployment for democratic discourse sentiment assessment. "Crisis Dynamics Learner" [23] employed multi-task learning integrating sentiment detection, emotion classification, intent prediction. Shared encoders supported representation reuse while attention layers focused on crisis-relevant cues. Subject-based intent modeling enhanced contextual discrimination.

"CSHET" [24] framework addressed bilingual social text containing alternating Hausa plus English expressions. Data preparation involved language identification at token level, normalization of mixed lexical forms, removal of script inconsistencies. Custom tokenization preserved semantic continuity across language boundaries. Shared embedding layers represented cross-lingual meaning within unified vector space. Deep neural classifiers learned sentiment cues embedded within mixed syntactic structures. "FRMS" [25] focused on separating sentiment-relevant information from heterogeneous multimodal inputs. Textual features plus visual representations were encoded through modality-specific networks. Feature disentanglement mechanisms isolated sentiment dimensions from auxiliary content factors. Reconstruction modules preserved semantic integrity within each modality. Joint optimization aligned latent spaces without redundancy leakage. Cross-modal consistency constraints ensured coherent sentiment representation.

Bio-inspired optimization has emerged as a powerful paradigm in intelligent system design, drawing inspiration from natural behaviors such as swarm coordination, evolutionary adaptation, and ecological competition [26]-[33]. Algorithms modeled on collective intelligence, adaptive search, and survival-driven selection have demonstrated strong capability in navigating high-dimensional and non-linear solution spaces. In text analytics and financial modeling contexts, such strategies support enhanced exploration–exploitation balance, parameter stability, and convergence robustness [34]-[45]. Optimization frameworks inspired by biological systems are particularly effective in handling noisy, dynamic, and temporally volatile environments, where traditional gradient-based tuning may struggle with local stagnation. Incorporating bio-inspired principles into sentiment-driven forecasting pipelines can improve hyperparameter calibration, adaptive weighting of objectives, and model generalization under rapidly shifting market signals [46]-[57]. This perspective complements transformer-based architectures by strengthening structural optimization and search efficiency in complex predictive ecosystems [58]-[63].

Existing literature predominantly focuses on sentiment classification, domain adaptation, bias auditing, or multimodal representation without integrating temporal market conditioning into a unified generative structure. Prior financial sentiment engines emphasize polarity extraction without structured multi-horizon forecasting. Multi-task learning studies address crisis or political discourse but lack volatility-aware temporal tagging. The proposed framework differs by embedding dynamic market-phase tags, employing

structured multi-field decoding within a single transformer backbone, and integrating horizon-separated directional outputs. Significance arises from measurable improvements across clustering fidelity, correlation strength, and detection reliability, establishing methodological advancement over sentiment-only or static financial prediction systems.

3. TEXT-TO-TEXT TRANSFER TRANSFORMER FINANCIAL CHRONOLOGICAL GENERATOR

Text-to-Text Transfer Transformer Financial Chronological Generator (T5-FinChronoGen) is a temporal tag–guided, multi-task text-to-text transformer framework that interprets tweet sentiment to generate time-aware stock direction forecasts and contextual financial explanations.

3.1. Tweet Market Synchronization and Metadata Extraction

Establishing the foundation for temporally guided multi-task learning in financial forecasting begins with precisely synchronizing social sentiment data with quantitative market indicators. Tweets represent retail investors' and market observers' spontaneous, unfiltered emotional responses. These textual fragments, though noisy, often encode early cues of market anxiety, excitement, or disillusionment. The model's ability to exploit such dynamics depends on aligning each tweet with real-time financial signals price fluctuations, trading volume surges, or volatility anomalies. Only through this pairing can temporal tags attain genuine relevance. Synchronization must also consider the intra-day variability of financial discourse, especially in environments where seconds can shift investor behavior.

To represent this alignment, a tweet-level association score can be defined to quantify how closely a tweet's posting time aligns with measurable market signals.

$$\phi_t = \lambda_1 \cdot \left(\frac{|P_t - P_{t-\delta}|}{P_{t-\delta}} \right) + \lambda_1 \cdot \left(\frac{V_t - \mu_V}{\sigma_V} \right) \quad (1)$$

P_t denotes the stock price at the tweet timestamp t, and $P_{t-\delta}$ refers to the immediate prior price window. V_t captures the trading volume at t, while μ_V and σ_V are the mean and standard deviation of volume within the session window. The coefficients λ_1 and λ_2 represent weight preferences for price and volume sensitivity, respectively. This composite score reflects how strongly a tweet is temporally anchored to observable financial activity.

Once synchronization is complete, further processing must interpret not just temporal positioning but also the emotional character of the tweet. Extracting sentiment-related cues from unstructured language requires mapping informal expressions, sarcasm, and euphemistic phrasing into polar structures. To formally convert the lexical elements into sentiment-bearing features, define a time-weighted polarity measure as:

$$\psi_s = \frac{1}{T_s} \sum_{i=1}^{T_s} \omega_i \cdot Pol(\omega_i) \quad (2)$$

In this formulation, T_s represents the total number of sentiment-bearing tokens ω_i in a tweet. Each token is associated with a function $Pol(\omega_i)$, which returns the sentiment polarity continuously from -1 to +1. The weight ω_i adjusts the influence of each token based on its location within the tweet or its intensity as determined by an attention-calibrated polarity lexicon. The resulting score reflects a soft sentiment average biased toward more influential words in the sentence structure.

Mapping tweet semantics into financial space requires sentiment decoding and event window detection. Market participants often react to corporate disclosures, earnings, and macroeconomic data, triggering coordinated social commentary bursts. Identifying these windows improves the credibility of temporal tagging. Define an event correlation score to estimate how tightly clustered a tweet is within such financial bursts:

$$\zeta_e = \frac{1}{N_e} \sum_{j=1}^{N_e} exp\left(-\gamma \left| t - t_j \right|\right) \quad (3)$$

N_e represents the number of tweets in the surrounding window, and t_j denotes their respective timestamps. The decay parameter γ controls how tightly the weighting collapses around t, highlighting whether the tweet falls into a market-wide narrative cluster. The higher this score, the more likely the tweet belongs to a high-impact sentiment episode.

Contextual signals improve further by embedding temporal states explicitly into each tweet's metadata. This includes variables for market

phase classification—pre-market, open session, or after-hours along with event flags for earnings days or macroeconomic releases. Formally, define a market-context vector Θ_t to collect these categorical signals:

$$\Theta_t = [\eta_m, \delta_a, k_n, \xi_f] \quad (4)$$

In this representation, η_m denotes market session (categorical: early, mid, late), δ_a signals asset-level volatility states, k_n encodes news-trigger relevance, and ξ_f represents forecast timing zone (short-range, intermediate, or long-range impact). These elements offer fine-grained control over how each tweet is interpreted contextually during input construction.

3.2. Dynamic Temporal Tag Generation from Market Signals

Temporal tags serve as structured linguistic carriers of financial timing that convert raw tweet–market alignment into meaningful contextual scaffolding. These tags do not merely denote time but encode market-specific states, volatility narratives, and investor mood transitions. Constructing such tags dynamically from real-world trading signals enables the model to interpret sentiment-bearing tweets precisely tuned to evolving financial rhythms. Relying on static or generic tags fails to reflect the subtlety of intraday sentiment flow. Instead, dynamic tags adaptively reflect the tweet's environment during a post-announcement decline, midday reversal, or pre-market optimism surge thereby improving contextual quality for downstream multi-task predictions.

To generate these temporal tags intelligently, the first step involves detecting latent market states over continuous financial streams. A dynamic tagging index can be constructed using volatility-aware market scoring that segments time into labeled intervals. Define this interval-specific temporal tag score as:

$$\tau_k = \alpha_1 \cdot \left(\frac{\sigma_k^{(P)}}{\sigma^{(P)}}\right) + \alpha_2 \cdot \left(\frac{\Delta_k^{(R)}}{max(\Delta^{(R)})}\right) \quad (5)$$

Here, $\sigma_k^{(P)}$ refers to the price volatility in segment k, while $\overline{\sigma^{(P)}}$ denotes its rolling average across all intervals. $\Delta_k^{(R)}$captures return fluctuation range within segment k, and $max(\Delta^{(R)})$ is the session-wide maximum return deviation. The parameters α_1 and α_2 govern the emphasis placed on volatility and return variability. This formulation identifies periods where tweet sentiment likely corresponds to market instability or investor overreaction.

Detecting shifts between financial states requires segment-wise scoring and temporal boundary selection. These boundaries act as dividers between calm and volatile phases, setting the label regime for tags. To establish an adaptive boundary threshold, define a change detection function as:

$$\Delta_\tau = \left|\frac{d}{dk}\tau_k\right| > \xi \quad (6)$$

The derivative $\frac{d}{dk}\tau_k$ measures the rate of change in the temporal tag score across segments. The threshold ξ functions as a volatility signal switch. When the rate of change exceeds ξ, a tag transition is triggered, e.g., from "early gain confidence" to "mid-session drop caution."

Constructing the tag label itself requires combining financial positioning with linguistic pattern alignment. Each tweet must inherit a phrase reflecting timing and underlying market conditions. The tag phrase θ_k^* can be generated using a rule-based composition function over indexed components:

$$\theta_k^* = Concat \begin{pmatrix} Session(k), TrendState(k), \\ SentimentCue(k) \end{pmatrix} \quad (7)$$

In this structure, $Session(k)$ identifies the market period label (e.g., pre-open, intraday, closing), $TrendState(k)$reflects directional momentum (bullish surge, recovery, drawdown), and $SentimentCue(k)$derives from tweet-polarity skew distributions captured within that interval. These three building blocks together produce dynamic, semantically precise tags such as "mid-session reversal optimism" or "post-decline uncertainty."

A comparative efficiency metric is required to determine whether a newly generated tag offers predictive strength over static alternatives. Define the temporal tag discriminative power (Υ) as:

$$\Upsilon = \frac{\mathbb{I}(\theta_k^*)}{\mathbb{I}(\theta_{static})} \quad (8)$$

Here, $I(\cdot)$ denotes the mutual information between the tag and true downstream outcomes (e.g., sentiment labels, price directions). A value $\Upsilon > 1$ confirms that the dynamic tag structure contributes

more contextual clarity than its static counterpart. This evaluative check ensures that each dynamic tag embeds meaningful signal strength for multi-task interpretation.

3.3. Time-Anchored Tweet Input Construction

Constructing the final input for the generative model involves embedding temporal context directly into the tweet stream, forming a semantically interpretable and financially coherent input sequence. This operation must preserve emotional nuance from the tweet text while augmenting it with chronological significance derived from dynamic tag generation. The resulting formulation enables the model to distinguish between sentiment that emerges during bullish surges and that which appears amidst sharp declines. Without this anchoring, sentiment-bearing inputs risk being misinterpreted or treated uniformly, undermining the market-specific logic that drives investor reactions.

To initiate input construction, a base encoding function is first defined, which fuses the dynamic temporal tag θ_k^* with the tweet's textual content T_i. This composite textual input X_i is created using a context-controlled concatenation as follows:

$$X_i = \theta_k^* \oplus [SEP] \oplus T_i \tag{9}$$

The operation $\oplus$ indicates concatenation with field-level separation, using a designated marker $[SEP]$ to signal the transition from tag to raw text. The tag θ_k^* originates from Eq.(7), while T_i captures the cleaned and normalized tweet. This formulation guarantees structural clarity for the encoder while ensuring the temporal anchor remains syntactically distinguishable.

Preserving semantic fidelity demands more than raw concatenation. Attention distribution across temporal and tweet segments must be regulated to prevent over-dominance by either portion. A segment-wise attention control vector a_i is applied over the token stream of X_i, defined as:

$$a_i = \left[\underbrace{\beta_1, \beta_1, \ldots\ldots}_{|\theta_k^*|}, \underbrace{\beta_2, \beta_2, \ldots}_{|T_i|} \right] \tag{10}$$

The parameter β_1 applies uniform weight across the temporal tag while β_2 does the same across tweet tokens. This balance controls how much influence each component carries in contextual embedding. The values are learnable and calibrated to preserve informational asymmetry where needed for example, emphasizing tagging context in volatile market regimes.

The token position is also crucial in enabling the encoder to distinguish the tag from the tweet structure. A dual-phase positional embedding schema p_i is applied to ensure the transformer retains awareness of logical text boundaries. This positional alignment is defined by:

$$p_i[j] = \begin{cases} j, & if\ j \le |\theta_k^*| \\ j + \delta, & if\ j > |\theta_k^*| \end{cases} \tag{11}$$

Here, j indexes each token position in the combined stream. The shift constant δ prevents positional overlap between tag and tweet, introducing structural clarity in attention computation during encoding. This positional strategy helps the model interpret relative position without confusion between tag-origin and tweet-origin tokens.

A lexical normalization layer is applied to optimize encoder-level readiness further, ensuring syntactic simplification and sentiment preservation. This layer transforms informal tweet text into a cleaned semantic vector I_i, constructed using a lexicon-weighted filter:

$$I_i = \sum_{t=1}^{|T_i|} \rho_t \cdot e_t \tag{12}$$

Here, e_t represents the embedding of token t in the tweet while ρ_t is the polarity-based relevance score extracted from sentiment lexicons. Tokens with higher emotional charge are amplified, guiding the encoder to focus on sentiment-rich expressions over neutral filler text.

Preserving sentiment integrity over multi-token phrases requires contextual reweighting through trigram scoring. A sentiment trigram strength function χ_i is defined to emphasize emotionally loaded phrase clusters:

$$\chi_i = \frac{1}{|G_i|} \sum_{g \in G_i} \zeta_g \cdot Polarity(g) \tag{13}$$

The set G_i contains all trigrams from tweet T_i, and ζ_g denotes the term strength based on co-occurrence frequency and phase polarity. This scoring enhances attention on cohesive emotional structures, especially when sarcastic, speculative, or speculative language emerges.

Final input readiness is validated through a tag-text coherence score, defined to ensure logical continuity between temporal framing and tweet content. Let Ω_i represent this alignment index:

$$\Omega_i = Sim(\theta_k^*, T_i) = \frac{\langle v_\theta, v_T \rangle}{\|v_\theta\| \cdot \|v_T\|} \quad (14)$$

The vectors v_θ and v_T represent sentence-level embeddings for the tag and tweet, respectively, while $\langle \cdot, \cdot \rangle$denotes the dot product. This cosine similarity confirms semantic compatibility, ensuring that tag and tweet do not diverge in topic or polarity before encoder ingestion.

3.4. Multi-Task Output String Encoding with Field Control

Multi-task prediction within financial sentiment frameworks demands a coordinated representation of outputs that can capture different dimensions of tweet-derived market insight. Each tweet, enriched through time-anchored input construction, carries latent information spanning emotional polarity, directional stock movement, and event causality. Each outcome component must be encoded into a single, well-structured output string to ensure efficient training and interpretable generation. This design simplifies decoder supervision, optimizes generation logic, and enables human-readable outputs suitable for downstream integration in real-world financial decision systems.

A unified output string Y_i is created through field-level composition, in which each task is mapped to a fixed position within the sequence. Let the output structure be formulated using a symbolically governed delimiter protocol:

$$Y_i = Field_1 \| Field_2 \| Field_3 \quad (15)$$

Here, ‖ indicates a structured delimiter (such as "|") that separates fields for sentiment classification, stock movement prediction, and event cause generation. Each field is mapped to a semantically constrained vocabulary range. This format ensures the model learns position-wise alignment between input signals and their corresponding multi-task targets.

Control over vocabulary usage within each field is implemented using task-wise decoding constraints. Define the output vocabulary allocation matrix V_{allo} , which regulates field-wise token prediction:

$$V_{alloc} = \begin{bmatrix} V_s & 0 & 0 \\ 0 & V_t & 0 \\ 0 & 0 & V_e \end{bmatrix} \quad (16)$$

In this matrix, $V_s, V_t,$ and V_e represent the vocabularies for sentiment labels, trend classes, and event descriptors, respectively. The zeros denote disallowed vocabularies for unrelated fields. This field-specific constraint mechanism ensures semantic clarity and prevents output ambiguity during decoding.

To verify the internal consistency of the generated output string, a structural alignment function k_i is applied, which penalizes misordered or malformed sequences. This function evaluates field alignment as follows:

$$k_i = \prod_{j=1}^{3} \delta(f_j, V_j) \quad (17)$$

Each f_j denotes the decoded token group corresponding to the j-th field, and $\delta(\cdot)$ is an indicator that returns 1 when the field content belongs entirely to the designated vocabulary V_j, else 0. A zero value of k_i signals an invalid structure, triggering a regeneration loop or output rejection logic during training.

Field richness is equally critical, particularly in the event description component, where generic tokens must be avoided. An information richness function Λ_i is applied over the event field to prioritize outputs containing domain-specific terms. This is expressed as:

$$\Lambda_i = \frac{1}{|T_e|} \sum_{w \in T_e} \tau_w \cdot 1(w \in f_3) \quad (18)$$

The set T_e represents the curated event vocabulary, τ_w is a term-specific domain informativeness score, and $1(\cdot)$ indicates the presence of the term in the third field. This function ensures lexical depth and interpretability, preventing overly generic outputs that fail to reflect market-specific language.

To balance learning dynamics across the three tasks embedded in the unified output string, a weighted field importance vector w_f is introduced to modulate gradient emphasis during training:

$$L_i = \sum_{j=1}^{3} w_j \cdot L(f_j, \hat{f}_j) \quad (19)$$

Each w_j corresponds to the weight for field j, allowing the model to learn from underrepresented or harder-to-predict tasks without destabilizing convergence. The function $L(f_j, \hat{f}_j)$ computes the

standard token-level cross-entropy loss between predicted and ground truth field content.

Consistency in output style across different training batches is critical for convergence. To enforce template-level regularity, a format encoding loss Δ_i is introduced. This loss penalizes variations from the fixed delimiter-structured style defined in Eq.(15) and is calculated as:

$$\Delta_i = \gamma \cdot \sum_{k \in misplaced} \big(1 - 1(k = \|)\big) \quad (20)$$

The constant γ governs the penalty strength, and the set misplaced captures token positions where delimiters were expected but incorrect tokens appeared. This regularisation term helps the decoder maintain a predictable structure, even when faced with ambiguous input-output mappings.

3.5 Tokenization and Field-Aligned Input–Output Pairing

Transforming structured sequences into model-digestible formats becomes a critical enabler for a multi-task generative framework designed to decode financial sentiment from social text. The temporal-tagged input and field-controlled output string must be represented as discrete token sequences, respecting structural boundaries, semantic alignment, and decoder expectations. Tokenization is not only a mechanical preprocessing step; it is the entry point for enforcing consistency, controlling sequence lengths, guiding positional encoding, and supporting lexical sensitivity across sentiment, market trends, and causal rationales. This stage binds the output grammar and temporal-aware input construction together to ensure coherent, field-aligned learning.

The tokenization of time-anchored input X_i, as defined in Eq.(9), is conducted using subword segmentation via a byte-pair encoding scheme. Let the tokenization function $T(\cdot)$ operate over the concatenated input stream, producing a token sequence x_i as:

$$x_i = T(\theta_k^* \oplus [SEP] \oplus T_i) \quad (21)$$

The input tokens x_i retain both the temporal structure and the semantic tone of the tweet. The segmentation captures entity fragments, financial phrases, and sentiment modifiers with higher fidelity than word-level boundaries. The $[SEP]$ token remains unsegmented, functioning as a hard demarcation marker during embedding and self-attention computations.

On the output side, the structured multi-task string Υ_i, previously defined in Eq.(15), is also segmented into decoder-friendly tokens using the same scheme. The tokenized output y_i is given by:

$$y_i = T(Field_1 \| Field_2 \| Field_3) \quad (22)$$

The output tokens preserve field ordering and maintain discrete task identity. The vocabulary preserves the delimiter symbol to guide the autoregressive decoder in transitioning between field zones during generation. This token control structure ensures that the model aligns each portion of its output with the proper segment of the target task.

Positional indexing is essential to keep the input-output mapping coherent over long sequences. Each token x_i^j in the input sequence x_i receives a unique index derived from a phase-sensitive positional embedding schema. Define this indexed matrix P_x for the input sequence as:

$$P_x[j] = \begin{cases} j, & if\ x_i^j \in \theta_k^* \\ j + \eta, & if\ x_i^j \in T_i \end{cases} \quad (23)$$

The positional offset η displaces tweet tokens to prevent overlap with the tag's positional domain. This maintains interpretive independence during encoding and avoids confusing temporal tokens with tweet-native tokens in self-attention layers.

For task-focused decoding, token-wise field mapping is introduced over the output tokens. This map F_j assigns every token in y_i to its field of origin, expressed as:

$$F_j = \begin{cases} s, & if\ y_i^j \in V_s \\ t, & if\ y_i^j \in V_t \\ e, & if\ y_i^j \in V_e \end{cases} \quad (24)$$

Each token's field affiliation enables field-wise attention control, auxiliary loss routing, and interpretability scoring. By maintaining this alignment, decoder heads can differentiate whether a generated token expresses emotional polarity, directional movement, or event rationale.

To quantify alignment quality between input semantics and field-specific output segments, define the field-level relevance score Ψ_j between tag-enriched input and output tokens:

$$\Psi_j = \frac{\sum_{k=1}^{|X_i|} Sim\big(x_i^k, y_i^j\big)}{|x_i|} \quad (25)$$

The similarity function $Sim(\cdot)$ evaluates embedding-level proximity between a specific output token y_i^j and the entire input sequence. This relevance quantifier is tracked across fields to assess how strongly sentiment tokens attend to emotional segments of the tweet or whether market direction terms reflect price-volatility keywords from the input.

During the batch construction phase, input-output token pairs are grouped, and each pair is checked for tag conformity using a syntax validation score. Define this syntactic coherence validator Γ_i as:

$$\Gamma_i = \prod_{q\in\{1,2,3\}} 1\big(Field_q \text{ is closed by } ||\big) \quad (26)$$

The indicator function ensures that each field ends at a delimiter boundary, preventing malformed sequences. A failure in this check flags the sample for augmentation, reformatting, or exclusion, maintaining syntactic reliability during autoregressive training.

3.6. Unified Output Generation through T5 Decoder

Unified decoding within a multi-task generative transformer necessitates a controlled yet flexible mechanism for sequential token emission that captures sentiment polarity, directional trend, and event rationale in a cohesive text output. The T5 decoder architecture is inherently autoregressive, allowing each token to be conditioned on the preceding ones. This step leverages that capability to sequentially construct multi-field predictions, where each portion of the output string adheres to its task-specific vocabulary and formatting constraints established in the previous field-controlled construction. The generation process must remain sensitive to temporal tag context, ensure field-level accuracy, and enforce semantic fluency from start to end.

The generation begins with the decoder receiving an encoder-derived context vector Z_i for each input token sequence x_i, defined previously in Eq.(21). Each decoder step t generates a token $\hat{y}_t$ by applying a probability distribution over the vocabulary, conditioned on the encoder outputs and the previously generated token sequence. The probability distribution over token $v \in V$ at time t is given by:

$$P(\hat{y}_t = v|\hat{y}_{<t}, Z_i) = softmax(W_o \cdot h_t + b_o) \quad (27)$$

Here, h_t is the decoder hidden State at step t, while W_o and b_o are the learnable output projection weights and biases. The softmax ensures that the predicted token $\hat{y}_t$ is selected based on its compatibility with both the prior token sequence and the encoded input.

To regulate field transitions during generation, a position-aware decoding mask M_t is applied at each step to prevent field leakage. This mask dynamically gates the eligible vocabulary tokens based on the active task field. The gating function can be described as:

$$M_t[v] = \begin{cases} 1, & if\ v \in V_{F_t} \\ 0, & otherwise \end{cases} \quad (28)$$

In this expression, $F_t$denotes the current field inferred from position t, as tracked using the delimiter structure defined in Eq.(22). The vocabulary subsets V_{F_t} represent permissible tokens for that specific field. Applying this mask maintains field fidelity throughout the generation.

Field-wise contextual recurrence is crucial for learning intra-field dependencies, especially within the event descriptor segment. A self-reinforcing attention module integrates previous token semantics through a recurrent context encoder r_t, which evolves as:

$$r_t = \sigma(W_r \cdot [h_{t-1}, e_{t-1}] + b_r) \quad (29)$$

The previous decoder state h_{t-1} and embedded token e_{t-1} are concatenated and passed through a recurrent transformation parameterized by W_r and b_r. The sigmoid function $\sigma(\cdot)$ ensures smooth context accumulation. This vector enriches decoding at step t, especially for longer event phrases where topic continuity matters.

To reinforce semantic alignment between the generated output and input tweet context, a joint attention map A_t is calculated between decoder step t and encoder outputs Z_i. This is modeled as:

$$A_t[j] = \frac{exp\big(h_t \cdot z_j\big)}{\sum_{k=1}^{|z_i|} exp(h_t \cdot z_k)} \quad (30)$$

Each z_j represents an encoded token vector from the input. The attention map $A_t$directs the decoder to the most relevant input tokens at each generation

step, especially when decoding sentiment or volatility-linked terms.

Fluency of output over the full sequence is monitored through an entropy stabilization measure ε_t, which penalizes token selections from overly flat or peaked probability distributions. This score is defined as:

$$\varepsilon_t = -\sum_{v \in V} P(\hat{y}_t = v) \cdot logP(\hat{y}_t = v) \quad (31)$$

Higher entropy indicates more token uncertainty, while lower values signal overconfidence or mode collapse. A stable entropy trajectory across tokens supports balanced generation, especially when transitioning between fields.

To support early stopping when a full output string has been generated successfully, a termination signal function Φ_i is employed, detecting the final delimiter sequence and evaluating field completeness. The signal is calculated as:

$$\Phi_i = 1(\exists t: \hat{y}_t = [END] \Lambda FieldsComplete(\hat{y}_{1:t})) \quad (32)$$

This binary function returns 1 when a valid end token is reached, and all required fields have been properly decoded using structural validation defined in Eq.(26). It prevents premature or incomplete string termination, guaranteeing full task coverage.

3.7. Composite Loss Calculation and Confidence Estimation

Effective optimization in a temporally grounded multi-task generative model hinges on the joint calibration of prediction accuracy and structural discipline across diverse fields. Each decoded token, as produced in the unified output string, must match the reference labels and align with the expected field boundaries and market semantics. In this context, a composite loss architecture becomes essential for balancing segment-level specificity with global generation consistency. This loss system must penalize intra-field errors, delimiter misplacement, and semantic ambiguity while offering confidence metrics that quantify the trustworthiness of each prediction especially valuable in financial scenarios where precision drives decision-making.

The base loss over the generated sequence $\hat{y}_i$and the reference sequence y_i, tokenised as described in Eq.(22), is computed using standard token-level cross-entropy. Let the primary generative loss function be defined as:

$$L_{gen} = -\sum_{t=1}^{|y_i|} logP(\hat{y}_t = y_t | \hat{y} < t, Z_i) \quad (33)$$

This loss penalizes deviations from the target tokens across the full sequence length. Each predicted token $\hat{y}_t$ is conditioned on all prior tokens and encoder context Z_i, as established in Eq.(27). The summation captures cumulative generative fidelity, encompassing all task fields embedded within the output string.

To modulate task-level contributions during learning, a field-aware loss distribution vector w_f is applied. This reweights the loss based on task complexity and label imbalance. Let the reweighted composite loss be described as:

$$L_{comp} = \sum_{j=1}^{3} w_j \cdot L_j \quad (34)$$

Each L_j represents the sub-loss computed over tokens belonging to field j sentiment, trend, and event. The weights w_j adjust the gradient impact of each task field, enhancing model flexibility in scenarios where one task may dominate or lag due to data skew.

Field structural compliance is encouraged using a boundary regularization penalty, ensuring the correct use of delimiters and preventing field overlap. Let the delimiter consistency loss be given by:

$$L_{delim} = \lambda_d \cdot \sum_{k \in D} 1(\hat{y}_k \neq \|) \quad (35)$$

The set D includes expected delimiter positions derived from the reference sequence structure. The indicator function flags incorrect token placements while λ_d controls the penalty magnitude. This loss ensures the decoder respects output field segmentation during generation.

An embedding similarity penalty is applied to incorporate field-level semantic control when generated field tokens deviate semantically from their intended task domain. Define the field mismatch loss as:

$$L_{mismatch} = \lambda_m \cdot \sum_{j=1}^{3} \sum_{t \in F_j} \left(1 - cos\left(e_t, c_j\right)\right) \quad (36)$$

For each field j, the embedding $e_t$corresponds to the generated token at position t, while c_j denotes the centroid embedding of the field's valid vocabulary. The cosine similarity promotes semantic coherence and task-appropriate lexical usage. The penalty strength λ_m ensures that off-topic tokens are discouraged during training.

Beyond loss, predictive confidence becomes a central interpretive feature, particularly in stock-related sentiment analysis where financial stakes are high. Define the token-wise confidence score C_t as the entropy-negated certainty of token generation:

$$C_t = 1 + \sum_{v \in V} P(\hat{y}_t = v) \cdot logP(\hat{y}_t = v) \quad (37)$$

This formulation rewards peak probability distributions that reflect high decoder certainty. Low-confidence tokens with flatter distributions receive values closer to zero. Token-wise confidences can later be aggregated across fields to assess which task sub-prediction carries more weight in decision contexts.

Field-wise confidence scores are computed by averaging over constituent tokens to support interpretability in post-inference decision systems. Let the field confidence vector C_j be given as:

$$C_f[j] = \frac{1}{|F_j|} \sum_{t \in F_j} C_t \quad (38)$$

Each component $C_f[j]$ represents the model's certainty in its prediction for task j. These values inform whether the generated sentiment, trend, or rationale can be trusted in sensitive forecasting operations such as position entry, portfolio rebalancing, or risk flagging.

A temperature-adjusted calibration function is introduced as confidence scores must remain calibrated across varying token distributions. This function $\tau(C_t)$ refines raw confidence values into scaled scores suited for thresholding:

$$\tau(C_t) = \frac{1}{1 + exp\left(-\gamma(C_t - \mu_C)\right)} \quad (39)$$

The parameter γ controls the sharpness of the transition and μ_C serves as the calibration midpoint. This non-linear transformation compresses extremes while expanding mid-confidence values, yielding smoother interpretive boundaries during downstream usage.

3.8. Ambiguity Resolution and Output Post-Validation

Multi-task generative outputs in financial sentiment interpretation demand careful post-validation to ensure task fidelity, domain accuracy, and clarity across all generated fields. Even under supervised field-constrained loss, generative decoding may occasionally yield syntactically correct yet semantically ambiguous outputs particularly when tweets include ironic tone, volatile emotional fluctuation, or disconnected financial cues. This ambiguity can lead to mismatches between model-generated sentiment labels and actual investor mood or misleading trend tags that conflict with temporal alignment. An output validation system, supplemented by ambiguity resolution scoring, acts as a secondary layer to detect, interpret, and correct such inconsistencies without compromising generation autonomy.

The first mechanism for ambiguity assessment quantifies lexical uncertainty using a trigram-level entropy bandpass. Let each generated sequence $\hat{y}_i$ be parsed into trigrams, and define the trigram entropy spread Υ_i as:

$$\Upsilon_i = \frac{1}{|G_i|} \sum_{g \in G_i} - \sum_{v \in V} P(v|g) log\ P(v|g) \quad (40)$$

Here, G_i denotes the set of all trigram spans within $\hat{y}_i$, and $P(v \mid g)$ is the conditional token distribution over the vocabulary V given the trigram context g. Higher values of Υ_i indicate contextually ambiguous or noisy phrases where the decoder exhibited indecision or shallow lexical anchoring, signaling a candidate for soft correction or contextual review.

A coherence segmentation ratio is defined for each task zone to separate true field prediction from cross-field contamination. Let the field coherence metric Γ_j compute the intra-field lexical consistency as:

$$\Gamma_j = \frac{\sum_{t \in F_j} \delta\left(y_t \in V_j\right)}{\left|F_j\right|} \quad (41)$$

Each $F_j$identifies the token indices belonging to the j-th task field, while $\delta\left(y_t \in V_j\right)$returns one if token $y_t$belongs to the correct vocabulary V_j, otherwise 0. Values of Γ_j close to 1 confirms lexical purity for that task segment. Lower values expose probable

semantic leakage or syntactic mixing, prompting structural re-evaluation or filtering operations.

A semantic polarity overlap function is used to detect phrase-level field misalignment to determine if conflicting polarity expressions coexist across sentiment and trend fields. Let the cross-field polarity conflict score $\Phi_{s,t}$ be defined as:

$$\Phi_{s,t} = Polarity(Field_1) \cdot Direction(Field_2) \quad (42)$$

The function $Polarity(\cdot)$ maps the sentiment label into a numeric space: negative as -1, neutral as 0, and positive as +1. Similarly, $Direction(\cdot)$ encodes stock trend direction as +1 for upward, -1 for downward, and 0 for flat. A value of $\Phi_{s,t} < 0$ indicates contradiction, such as a positive sentiment co-occurring with a predicted downtrend, prompting manual or automated flagging for output rejection or rerouting.

Structural completeness is enforced by evaluating field and delimiter counts in the decoded output. Let the output completeness validator Ω_i count field segments, defined as:

$$\Omega_i = 1(count(\|, \hat{y}_i) = 2) \cdot \prod_{j=1}^{3} 1(|F_j| > 0) \quad (43)$$

The delimiter count function confirms two separators in the decoded string, segmenting it into three fields. Each $1(|F_j| > 0)$ ensures that none of the task outputs are empty or skipped during decoding. A value of $\Omega_i = 1$implies syntactic and positional completeness; otherwise, the sequence is discarded or regenerated.

A field re-annotation likelihood is computed using a recovery classifier trained on high-quality field-tagged data to determine whether ambiguous outputs are salvageable. Define the recoverability score Ψ_i as:

$$\Psi_i = \frac{1}{3}\sum_{j=1}^{3} P_{rec}(F_j \to V_j) \quad (44)$$

The probability $P_{rec}(F_j \to V_j)$ is obtained from a trained validation model that estimates whether the tokens in F_j could have plausibly originated from the correct field's vocabulary and semantic cluster. High values of Ψ_i indicate that field realignment might restore integrity without requiring full regeneration.

3.9. Deployment Inference with Horizon Forecasting Extension

A generative system must transition from experimental decoding to structured, horizon-specific inference for practical utility in financial markets. Market sentiment often evolves over layered time intervals, particularly when extracted from public social signals. Predictive accuracy alone is insufficient unless outputs are temporally anchored and tailored to various decision-making horizons. This step operationalizes T5-FinChronoGen in deployment settings by incorporating forecast horizon calibration, live tag embedding, and temporal span-sensitive output decomposition. Such a mechanism enables forecasts across short-term, medium-range, and event-conditioned temporal scales, aligning sentiment outputs with trading intentions such as scalping, swing holding, or momentum filtering.

To initiate horizon-aware inference, a timestamped tweet T_i^t is passed through a tag embedding selector that dynamically generates the most appropriate temporal descriptor θ_k^t, considering the proximity to market triggers. The resulting temporal-tagged input $\tilde{X}_i$ is constructed as:

$$\tilde{X}_i = \theta_k^t \oplus [SEP] \oplus T_i^t \quad (45)$$

Here, θ_k^t captures the market rhythm using session metadata, volatility snapshots, or earnings proximity. The $\oplus$ operator defines structured input fusion between tag and tweet, as carried over from the formulation in Eq.(9). This ensures that the inference pipeline remains robustly grounded in real-time temporal semantics even under dynamic financial stimuli.

The encoded input $\tilde{X}_i$ is processed by the trained encoder, and the decoder begins autoregressive generation of the output string $\tilde{Y}_i$. Under multi-horizon forecasting mode, the decoder is prompted to emit outputs structured with nested forecast spans. Define the decoded output as:

$$\tilde{Y}_i = Field_1 \| Field_{2,1h} \| Field_{2,1d} \| Field_3 \quad (46)$$

The segment $Field_{2,1h}$ corresponds to price direction forecast over the short-term (e.g., 1 hour), while $Field_{2,1d}$ captures anticipated movement across a longer duration (e.g., 1 day). This expansion from Eq.(15) accommodates multiple volatility response windows and allows the model to reflect the layered structure of trader attention.

To handle multi-span decoding, a nested delimiter map D_{multi} is introduced. This controls both field-level and horizon-level output ordering during inference. The map is constructed as follows:

$$D_{multi} = \{Field_1 \rightarrow V_s, Field_{2,1h} \rightarrow V_t^{(1h)}, Field_{2,1d} \rightarrow V_t^{(1d)}, Field_3 \rightarrow V_e\} \quad (47)$$

Each output zone is linked to a domain-specific vocabulary with $V_t^{(1h)}$ and $V_t^{(1d)}$representing specialized lexicons for immediate and delayed price shifts. These allocations constrain the decoder to produce horizon-appropriate directional cues, enhancing interpretability and decision confidence in downstream trading applications.

To enable time-segmented evaluation of forecast reliability, each horizon-specific token segment is post-processed through a confidence interpolator. Define the temporal confidence vector $C_h$as:

$$C_h[k] = \frac{1}{|f_{2,k}|} \sum_{t \in f_{2,k}} \tau(C_t) \quad (48)$$

The notation $f_{2,k}$ identifies token indices within the k-th trend forecast window (e.g., one h or 1d). The function $\tau(C_t)$, introduced in Eq.(39), transforms raw confidence scores into interpretable values for comparison. A higher value of $C_h[k]$ confirms stronger model trust in the trend forecast across the specified temporal window.

Actionability of predictions in live deployment hinges on post-decoding filtering and ranking. A forecast utility index Ξ_i is constructed using a joint field-confidence map, synthesizing sentiment polarity, short-term direction, and rationale certainty. The index is given by:

$$\Xi_i = \omega_s \cdot C_f[1] + \omega_{t1} \cdot C_h[1h] + \omega_e \cdot C_f[3] \quad (49)$$

The weights ω_s, ω_{t1}, and ω_e reflect the relative priority of sentiment, immediate trend, and explanation confidence in a live execution context. Scores from this index are applied to rank prediction sets or trigger conditional strategies within trading models or alerting systems.

A final tag-output alignment trace is generated to match the inferred output against the input tag's semantic intent to ensure interpretability for human analysts or regulatory oversight. Let the alignment trace ρ_i be expressed as:

$$\rho_i = cos\left(v_{\hat{Y}_i}, v_{\theta_k^t}\right) \quad (50)$$

The vectors $v_{\hat{Y}_i}$ and $v_{\theta_k^t}$ represent sentence embeddings of the decoded output and the original temporal tag. A high cosine similarity confirms that the decoder has remained faithful to the temporally conditioned input, avoiding drift or hallucination during sequence generation. Table 1. Exhibits the overall functionals of T5-FCG as Pseudocode

Table 1: Pseudocode for T5-FCG

```
Function T5-FinChronoGen(Tweets, MarketData):

  CleanedTweets ← CleanAndNormalize(Tweets)
  SyncedTweets ← AlignWithMarket(CleanedTweets, MarketData)
  TemporalTags ← GenerateTags(SyncedTweets, MarketData)
  InputSeq ← ConstructTaggedInput(TemporalTags, CleanedTweets)
  OutputSeq ← FormatOutput(SentimentLabels, TrendLabels, EventReasons)
  TokenizedInput ← Tokenize(InputSeq)
  TokenizedOutput ← Tokenize(OutputSeq)
  Model ← TrainT5Model(TokenizedInput, TokenizedOutput)

  For each NewTweet:
     Tag ← GenerateLiveTag(NewTweet, MarketSnapshot)
     Input ← Tokenize(Tag + NewTweet)
     Prediction ← GenerateOutput(Model, Input)
     Validated ← ValidateOutput(Prediction)
     Confidence ← ComputeConfidence(Prediction)
     Ranked ← RankPrediction(Prediction, Confidence)
     Display(Ranked)

End Function
```

4. DATASET DESCRIPTION

The dataset titled *Stock Tweets for Sentiment Analysis and Prediction* comprises over 580,000 tweets related to financial markets, tagged with sentiment polarity positive, neutral, or negative. Each entry contains tweet content, timestamp, and sentiment label, offering temporal alignment with market-relevant discourse. The dataset reflects high-frequency investor opinions, making it suitable for tasks involving sentiment classification, trend forecasting, and context-aware financial analysis. Linguistic diversity, informal expressions,

and domain-specific terms within the tweets simulate real-world trading sentiment. Time-based filtering enables structured segmentation for multi-horizon modeling. This dataset serves as a rich source for learning emotional cues, understanding crowd psychology, and developing generative systems that interpret market-sensitive language patterns.

5. RESULTS AND DISCUSSIONS

Results and discussions represent the interpretive analysis of measured performance metrics after model evaluation. This stage focuses on identifying how effectively a system classifies input data and the quality of those classifications under specific criteria. In this context, Classification Accuracy and F-Measure are two critical indicators of predictive quality. Classification Accuracy reflects the proportion of correctly predicted instances among all predictions, measuring overall correctness. F-Measure combines precision and recall, capturing the balance between how many relevant instances are retrieved and how many retrieved instances are relevant.

The Classification Accuracy values recorded for CSHET, FRMS, and T5-FCG are 51.483%, 58.797%, and 73.328% respectively. This progressive improvement highlights a clear gain in prediction correctness through T5-FCG's unified architecture. F-Measure follows a similar trend, with scores of 52.313 for CSHET, 60.170 for FRMS, and 75.446 for T5-FCG, reflecting enhanced balance between false positives and false negatives. Figure 1 consolidates these comparisons, illustrating the superiority of the T5-FCG model in capturing accurate, task-aligned sentiment patterns from tweets. This performance reflects stronger generalization and contextual understanding in tweet-driven stock market forecasting.

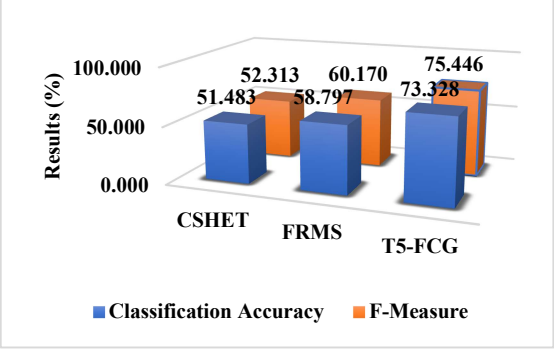


Figure 1: Classification Accuracy and F-Measure

Fowlkes-Mallows Index and Matthews Correlation Coefficient are two robust metrics that reveal clustering fidelity and predictive strength, particularly when datasets are imbalanced or contain complex linguistic structures. Fowlkes-Mallows Index measures the geometric mean between precision and recall, focusing on the similarity between actual and predicted class memberships. Matthews Correlation Coefficient evaluates the correlation between predicted and actual classifications, incorporating all outcomes including true positives, true negatives, false positives, and false negatives into a single coefficient.

Fowlkes-Mallows Index values for CSHET, FRMS, and T5-FCG are 52.434, 60.395, and 75.501, respectively, with noticeable improvement in clustering accuracy under the T5-FCG framework. This increase highlights better alignment between predicted and actual sentiment structures, particularly in cases involving emotionally dense tweet data. Matthews Correlation Coefficient scores follow a similar upward trend 3.431 for CSHET, 18.440 for FRMS, and 46.510 for T5-FCG indicating that T5-FCG captures sentiment logic and directional correctness more effectively. Figure 2 presents this progression, emphasizing the strong generalization and structural consistency achieved through temporally grounded, multi-task generation.

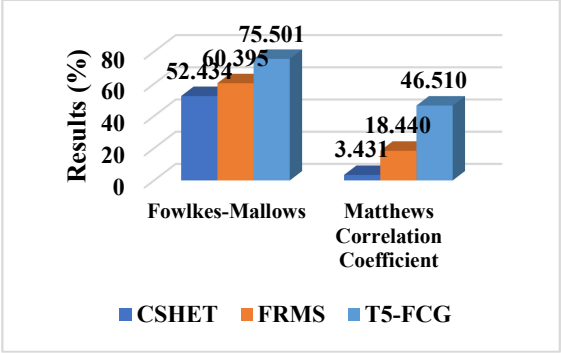


Figure 2: Fowlkes-Mallows Index and Matthews Correlation Coefficient

Precision and Recall are fundamental metrics used to evaluate classification performance, particularly in contexts involving imbalanced classes and high sensitivity to misclassification. Precision refers to the proportion of correctly identified positive predictions out of all predicted positives, capturing the model's ability to avoid false positives. Recall measures the proportion of

correctly identified positive instances out of all actual positives, reflecting how effectively the model identifies relevant sentiment expressions.

In the observed comparison, CSHET yields a Precision of 48.984 and Recall of 56.128, showing modest ability to isolate true sentiment from noise. FRMS improves these values to 55.392 for Precision and 65.850 for Recall, indicating better filtration and relevance detection. T5-FCG achieves the highest values, with 72.678 for Precision and 78.434 for Recall. This demonstrates that T5-FCG not only identifies tweet sentiments with greater accuracy but also reduces false alarms. Figure 3 highlights this enhancement, validating the model's capacity to capture high-confidence sentiment while retaining coverage. The combination of precision-focused structure and temporal conditioning enables the system to respond effectively to emotionally charged financial language.

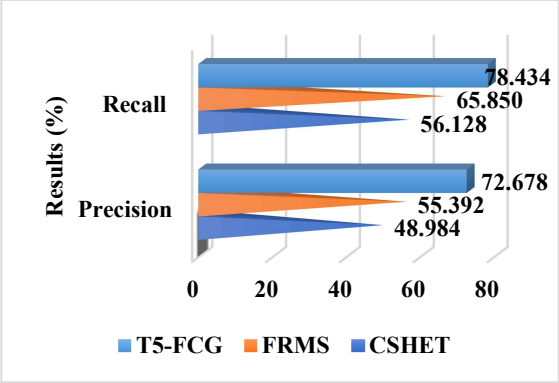


Figure 3: Precision and Recall

Detection-related metrics offer critical insight into how well a classification model distinguishes between true and false outcomes. Average Detection Rate, Miss Detection Rate, and Detection Rate serve as indicators of accuracy, failure avoidance, and overall detection capability. Average Detection Rate reflects the mean ability to detect both positive and negative classes correctly. Miss Detection Rate represents the proportion of actual positive cases that the model fails to identify, while Detection Rate corresponds to the proportion of overall correct detections across all instances.

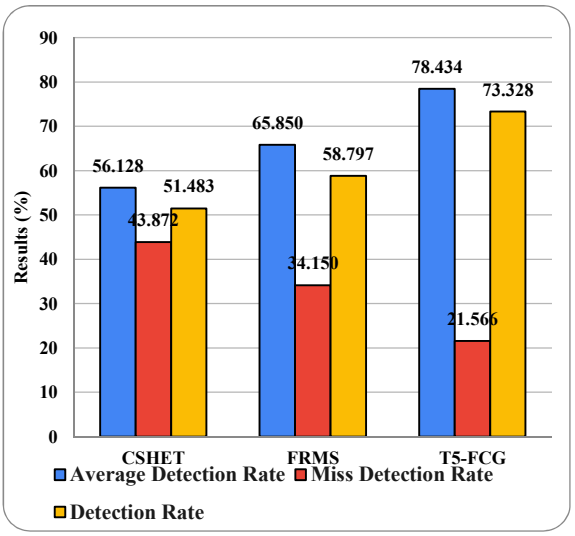


Figure 4: Average Detection Rate, Miss Detection Rate and Detection Rate

In the observed analysis, CSHET demonstrates an Average Detection Rate of 56.128, Miss Detection Rate of 43.872, and Detection Rate of 51.483, revealing limitations in its detection reliability. FRMS shows improved performance with an Average Detection Rate of 65.850, Miss Detection Rate of 34.150, and Detection Rate of 58.797, indicating a reduced rate of missed predictions. T5-FCG surpasses both models with an Average Detection Rate of 78.434, Miss Detection Rate of only 21.566, and Detection Rate of 73.328. These results, visualized in Figure 4, confirm that the temporally conditioned, multi-task generation in T5-FCG ensures fewer misclassifications and higher identification accuracy of market-relevant sentiment patterns in tweets.

Beyond performance gains, certain unintended observations emerged during evaluation. Temporal tagging occasionally amplified short-lived sentiment bursts that did not translate into sustained price movement, particularly under low-liquidity intervals. This indicates heightened sensitivity to micro-volatility clusters. Comparative benchmarking against CSHET and FRMS demonstrates consistent superiority across Accuracy, F-Measure, MCC, and detection metrics, reflecting stronger contextual generalization. Unlike prior models that operate on sentiment isolation, the proposed framework integrates temporal alignment and structured multi-task decoding, yielding measurable gains in correlation-based robustness. The improvement margin across all metrics indicates structural advancement rather than marginal optimization,

confirming enhanced interpretability and stability in volatile financial language environments.

From an industry perspective, the proposed architecture supports real-time financial monitoring systems, algorithmic trading dashboards, and institutional sentiment analytics platforms. Temporal tagging enables integration with live market feeds, allowing trading engines to differentiate between pre-market optimism, intra-session volatility, and post-event reactions. Multi-horizon directional forecasting supports scalping strategies, swing trading evaluation, and volatility hedging frameworks. Structured explanation generation enhances regulatory transparency and analyst interpretability. Financial institutions leveraging social signal analytics can incorporate this model into risk surveillance modules, portfolio sentiment overlays, and automated alert systems, strengthening market responsiveness under high-frequency information environments.

Despite its performance improvements, the framework exhibits certain limitations. Dependence on accurate market synchronization may introduce noise under irregular trading conditions or delayed data feeds. High sensitivity to short-term volatility clusters may exaggerate micro-sentiment fluctuations. The model operates on textual inputs only and does not incorporate numerical technical indicators or macroeconomic variables within the decoder structure. Computational complexity associated with multi-task generative decoding increases inference latency under large-scale deployment. Future work may explore multimodal fusion and adaptive volatility smoothing to mitigate these constraints.

The objectives of this study focused on temporally anchored sentiment interpretation, unified multi-task decoding, and horizon-aware stock direction forecasting within a single generative transformer framework. In contrast, prior studies in literature primarily concentrate on isolated sentiment classification, domain adaptation, clustering enhancement, or bias auditing without integrating dynamic market-phase conditioning into a structured forecasting pipeline. Reported works such as CSHET and FRMS demonstrate moderate improvements in polarity recognition; however, they lack synchronized market tagging and structured multi-field generation. The proposed framework achieves substantially higher Accuracy (73.328%), F-Measure (75.446), MCC (46.510), and Detection Rate (73.328), indicating stronger contextual generalization and correlation robustness. These measurable gains reflect fulfillment of the stated objectives, particularly the integration of temporal awareness and unified decoding. The contribution extends beyond performance improvement, establishing a methodological shift from sentiment-only modeling toward temporally grounded, multi-horizon generative financial forecasting.

5. CONCLUSION

Financial sentiment prediction using social media discourse has emerged as a vital domain in market-aware analytics. The dynamic and emotionally charged nature of tweets demands architectures capable of understanding language under temporal, contextual, and structural variations. A text-to-text generative framework, conditioned through temporal tagging and guided by task-specific decoding, enables the mapping of informal sentiment into structured financial insights. Incorporating temporal context into tweet interpretation strengthens the relationship between market conditions and public emotion. Multi-task generation allows the simultaneous decoding of sentiment, directional movement, and event relevance, enriching the semantic value of each prediction. Structuring outputs with field-level separation and validating content through post-processing ensures interpretability and model trustworthiness. By bridging emotional tone, market timing, and task logic, the proposed approach supports responsive forecasting systems suitable for high-frequency environments. Such a design contributes toward building reliable sentiment-intelligent financial interfaces that understand both what is being said and when it becomes significant, fostering stronger alignment between language-driven signals and strategic financial decision systems.

REFERENCES:

[1]. W. Ma and S. Y. Ho, “Sentiment-devoid lexicons: A novel method for domain-specific textual analysis in business and governance documents,” Information & Management, vol. 62, no. 1, p. 104055, 2025, doi: https://doi.org/10.1016/j.im.2024.104055.

[2]. Suzuki, Y. Ishikawa, M. Teraguchi, and H. Sakaji, “Sentiment works in small-cap stocks: Japanese stock’s sentiment with language models,” International Journal of Information Management Data Insights, vol. 5, no. 1, p.

100318, 2025, doi: https://doi.org/10.1016/j.jjimei.2024.100318.

[3]. S. AlMuhaideb, Y. AlNegheimish, T. AlOmar, R. AlSabti, M. AlKathery, and G. AlOlyyan, "Analyzing Arabic Twitter-Based Patient Experience Sentiments Using Multi-Dialect Arabic Bidirectional Encoder Representations from Transformers," Computers, Materials and Continua, vol. 76, no. 1, pp. 195–220, 2023, doi: https://doi.org/10.32604/cmc.2023.038368.

[4]. R. Moura, J. Carvalho, A. Plastino, and A. Paes, "Less is more: Pruning BERTweet architecture in Twitter sentiment analysis," Inf Process Manag, vol. 61, no. 4, p. 103688, 2024, doi: https://doi.org/10.1016/j.ipm.2024.103688.

[5]. X. Chen, H. Xie, Z. Li, H. Zhang, X. Tao, and F. L. Wang, "Sentiment analysis for stock market research: A bibliometric study," Natural Language Processing Journal, vol. 10, p. 100125, 2025, doi: https://doi.org/10.1016/j.nlp.2025.100125.

[6]. Z. Shao, X. Yao, F. Chen, Z. Wang, and J. Gao, "Revisiting time-varying dynamics in stock market forecasting: A multi-source sentiment analysis approach with large language model," Decis Support Syst, vol. 190, p. 114362, 2025, doi: https://doi.org/10.1016/j.dss.2024.114362.

[7]. I Tejaswini, V. G. Ganivada, and A. S. Muttipati, "Hateful tweet detection using a BiLSTM-BiGRU: An ensemble perspective," Entertain Comput, vol. 55, p. 101019, 2025, doi: https://doi.org/10.1016/j.entcom.2025.101019

[8]. V. Davydova, H. Yang, and E. Tutubalina, "Data and models for stance and premise detection in COVID-19 tweets: Insights from the Social Media Mining for Health (SMM4H) 2022 shared task," J Biomed Inform, vol. 149, p. 104555, 2024, doi: https://doi.org/10.1016/j.jbi.2023.104555.

[9]. R.S. de Oliveira and E. G. S. Nascimento, "Transformer-based large language foundation models for text generation: A comprehensive literature review for different languages and application domains," Inf Process Manag, vol. 63, no. 2, Part B, p. 104477, 2026, doi: https://doi.org/10.1016/j.ipm.2025.104477.

[10]. K. K. Sampath and M. Supriya, "Transformer Based Sentiment Analysis on Code Mixed Data," Procedia Comput Sci, vol. 233, pp. 682–691, 2024, doi: https://doi.org/10.1016/j.procs.2024.03.257.

[11]. S. Aslan, "A deep learning-based sentiment analysis approach (MF-CNN-BILSTM) and topic modeling of tweets related to the Ukraine–Russia conflict," Appl Soft Comput, vol. 143, p. 110404, 2023, doi: https://doi.org/10.1016/j.asoc.2023.110404.

[12]. A. Motwakel et al., "Sine Cosine Optimization with Deep Learning-Based Applied Linguistics for Sentiment Analysis on COVID-19 Tweets," Computers, Materials and Continua, vol. 75, no. 3, pp. 4767–4783, 2023, doi: https://doi.org/10.32604/cmc.2023.034840.

[13]. N. Nandal, R. Tanwar, and A.-S. K. Pathan, "Sentiment Analysis based Emotion Extraction for COVID-19 Using Crawled Tweets and Global Statistics for Mental Health," Procedia Comput Sci, vol. 218, pp. 949–958, 2023, doi: https://doi.org/10.1016/j.procs.2023.01.075.

[14]. B. Ogbuokiri et al., "Cross-domain fairness audit of sentiment label bias in foundation models: Comparing human and machine annotations on tweets and reviews," Machine Learning with Applications, vol. 21, p. 100717, 2025, doi: https://doi.org/10.1016/j.mlwa.2025.100717.

[15]. N. S. Mullah, W. M. N. W. Zainon, and M. N. Ab Wahab, "Transfer learning approach for identifying negative sentiment in tweets directed to football players," Eng Appl Artif Intell, vol. 133, p. 108377, 2024, doi: https://doi.org/10.1016/j.engappai.2024.108377.

[16]. M. Wilksch and O. Abramova, "PyFin-sentiment: Towards a machine-learning-based model for deriving sentiment from financial tweets," International Journal of Information Management Data Insights, vol. 3, no. 1, p. 100171, 2023, doi: https://doi.org/10.1016/j.jjimei.2023.100171.

[17]. A. M. Fashakh, M. Çevik, Ş. K. Aydoğan, and A. A. Ibrahim, "Detection cyberbullying using AI and sentiment analysis to examine psychological impacts on vulnerable groups," Egyptian Informatics Journal, vol. 32, p. 100856, 2025, doi: https://doi.org/10.1016/j.eij.2025.100856.

[18]. A. Alotaibi, A. Almutarie, S. Alotaibi, and M. Alotaibi, "Improving Fashion Sentiment Detection on X through Hybrid Transformers and RNNs," Computers, Materials and Continua, vol. 84, no. 3, pp. 4451–4467,

2025, doi: https://doi.org/10.32604/cmc.2025.066050.
[19]. M. Maghsoudi, N. Mohammadi, and M. Bakhtiari, "A novel approach to customer segmentation for product development on social media data: integrating aspect-based sentiment analysis and text mining," Knowl Based Syst, vol. 328, p. 114269, 2025, doi: https://doi.org/10.1016/j.knosys.2025.114269.
[20]. J. A. Aquino, D. J. Liew, and Y.-C. Chang, "Graph-aware pre-trained language model for political sentiment analysis in Filipino social media," Eng Appl Artif Intell, vol. 146, p. 110317, 2025, doi: https://doi.org/10.1016/j.engappai.2025.110317.
[21]. S. R. Kunam, M. S. Bhupal rao, M. R. Babu, and P. N. S. Kumar, "A sophisticated semantic analysis framework using an intelligent tweet data clustering and classification methodologies," Microprocess Microsyst, vol. 98, p. 104793, 2023, doi: https://doi.org/10.1016/j.micpro.2023.104793.
[22]. A. Khan, H. Zhang, N. Boudjellal, A. Ahmad, and M. Khan, "Improving Sentiment Analysis in Election-Based Conversations on Twitter with ElecBERT Language Model," Computers, Materials and Continua, vol. 76, no. 3, pp. 3345–3361, 2023, doi: https://doi.org/10.32604/cmc.2023.041520.
[23]. P. Y. Win Myint, S. L. Lo, and Y. Zhang, "Unveiling the dynamics of crisis events: Sentiment and emotion analysis via multi-task learning with attention mechanism and subject-based intent prediction," Inf Process Manag, vol. 61, no. 4, p. 103695, 2024, doi: https://doi.org/10.1016/j.ipm.2024.103695.
[24]. Y. Aliyu, A. Sarlan, K. U. Danyaro, A. Sani abd Rahman, A. A. Muazu, and M. Y. Abubakar, "Deep learning techniques for sentiment analysis in code-switched Hausa-English tweets," International Journal of Information Management Data Insights, vol. 5, no. 1, p. 100330, 2025, doi: https://doi.org/10.1016/j.jjimei.2025.100330.
[25]. Y. Fu, B. Huang, Y. Wen, and P. Zhang, "FDR-MSA: Enhancing multimodal sentiment analysis through feature disentanglement and reconstruction," Knowl Based Syst, vol. 297, p. 111965, 2024, doi: https://doi.org/10.1016/j.knosys.2024.111965.
[26]. J. Ramkumar and R. Vadivel, "Improved frog leap inspired protocol (IFLIP) – for routing in cognitive radio ad hoc networks (CRAHN)," World J. Eng., vol. 15, no. 2, pp. 306–311, 2018, doi: 10.1108/WJE-08-2017-0260.
[27]. J. Ramkumar and R. Vadivel, "Improved Wolf prey inspired protocol for routing in cognitive radio Ad Hoc networks," Int. J. Comput. Networks Appl., vol. 7, no. 5, pp. 126–136, 2020, doi: 10.22247/ijcna/2020/202977.
[28]. K. S. J. Marseline, J. Ramkumar, and D. R. Medhunhashini, "Sophisticated Kalman Filtering-Based Neural Network for Analyzing Sentiments in Online Courses," in Smart Innovation, Systems and Technologies, A. K. Somani, A. Mundra, R. K. Gupta, S. Bhattacharya, and A. P. Mazumdar, Eds., Springer Science and Business Media Deutschland GmbH, 2024, pp. 345–358. doi: 10.1007/978-981-97-3690-4_26.
[29]. L. Mani, S. Arumugam, and R. Jaganathan, "Performance Enhancement of Wireless Sensor Network Using Feisty Particle Swarm Optimization Protocol," in ACM International Conference Proceeding Series, Association for Computing Machinery, 2022. doi: 10.1145/3590837.3590907.
[30]. J. Ramkumar and R. Vadivel, "CSIP—cuckoo search inspired protocol for routing in cognitive radio ad hoc networks," in Advances in Intelligent Systems and Computing, D. P. Mohapatra and H. S. Behera, Eds., Springer Verlag, 2017, pp. 145–153. doi: 10.1007/978-981-10-3874-7_14.
[31]. N. K. Ojha, A. Pandita, and J. Ramkumar, "Cyber security challenges and dark side of AI: Review and current status," in Demystifying the Dark Side of AI in Business, IGI Global, 2024, pp. 117–137. doi: 10.4018/979-8-3693-0724-3.ch007.
[32]. [27]. R. Jaganathan, S. Mehta, and R. Krishan, Intelligent Decision Making Through Bio-Inspired Optimization. IGI Global, 2024. doi: 10.4018/979-8-3693-2073-0.
[33]. J. Ramkumar, K. S. Jeen Marseline, and D. R. Medhunhashini, "Relentless Firefly Optimization-Based Routing Protocol (RFORP) for Securing Fintech Data in IoT-Based Ad-Hoc Networks," Int. J. Comput. Networks Appl., vol. 10, no. 4, pp. 668–687, 2023, doi: 10.22247/ijcna/2023/223319.
[34]. M. P. Swapna and J. Ramkumar, "Multiple Memory Image Instances Stratagem to Detect Fileless Malware," in Communications in Computer and Information Science, S. Rajagopal, K. Popat, D. Meva, and S. Bajeja,

Eds., Springer Science and Business Media Deutschland GmbH, 2024, pp. 131–140. doi: 10.1007/978-3-031-59100-6_11.

[35]. [30]. M. Lingaraj, T. N. Sugumar, C. S. Felix, and J. Ramkumar, "Query aware routing protocol for mobility enabled wireless sensor network," Int. J. Comput. Networks Appl., vol. 8, no. 3, pp. 258–267, 2021, doi: 10.22247/ijcna/2021/209192.

[36]. S. P. Geetha, N. M. S. Sundari, J. Ramkumar, and R. Karthikeyan, "Energy Efficient Routing In Quantum Flying Ad Hoc Network (Q-FANET) Using Mamdani Fuzzy Inference Enhanced Dijkstra's Algorithm (MFI-EDA)," J. Theor. Appl. Inf. Technol., vol. 102, no. 9, pp. 3708–3724, 2024.

[37]. R. Jaganathan, S. Mehta, and R. Krishan, Bio-Inspired intelligence for smart decision-making. IGI Global, 2024.

[38]. R. Jaganathan and V. Ramasamy, "Performance modeling of bio-inspired routing protocols in Cognitive Radio Ad Hoc Network to reduce end-to-end delay," Int. J. Intell. Eng. Syst., vol. 12, no. 1, pp. 221–231, 2019.

[39]. J. Ramkumar, R. Vadivel, and B. Narasimhan, "Constrained Cuckoo Search Optimization Based Protocol for Routing in Cloud Network," Int. J. Comput. Networks Appl., vol. 8, no. 6, pp. 795–803, 2021.

[40]. J. Ramkumar, R. Karthikeyan, and M. Lingaraj, "Optimizing IoT-Based Quantum Wireless Sensor Networks Using NM-TEEN Fusion of Energy Efficiency and Systematic Governance," in Lecture Notes in Electrical Engineering, V. Shrivastava, J. C. Bansal, and B. K. Panigrahi, Eds., Springer Science and Business Media Deutschland GmbH, 2025, pp. 141–153.

[41]. B. Suchitra, R. Karthikeyan, J. Ramkumar, and V. Valarmathi, "Enhancing Recurrent Neural Network Performance for Latent Autoimmune Diabetes Detection (Lada) Using Exocoetidae Optimization," J. Theor. Appl. Inf. Technol., vol. 103, no. 5, pp. 1645–1667, 2025.

[42]. J. Ramkumar and D. Ravindran, "Machine learning and robotics in urban traffic flow optimization with graph neural networks and reinforcement learning," in Machine Learning and Robotics in Urban Planning and Management, 2025, pp. 83–104.

[43]. R. Jaganathan, K. Rajendran, and P. S. Ponnukumar, "Peregrine Falcon Optimization Routing Protocol (PFORP) for Achieving Ultra-Low Latency and Boosted Efficiency in 6G Drone Ad-Hoc Networks (DANET)," Int. J. Comput. Digit. Syst., vol. 17, no. 1, pp. 1–18, 2025.

[44]. S. P. Priyadharshini, F. Nirmala Irudayam, and J. Ramkumar, "An Unique Overture of Plithogenic Cubic Overset, Underset and Offset," in Studies in Fuzziness and Soft Computing, vol. 435, 2025, pp. 139–156.

[45]. [40]. J. Ramkumar, B. Varun, V. Valarmathi, D. R. Medhunhashini, and R. Karthikeyan, "Jaguar-Based Routing Protocol (JRP) For Improved Reliability And Reduced Packet Loss In Drone Ad-Hoc Networks (DANET)," J. Theor. Appl. Inf. Technol., vol. 103, no. 2, pp. 696–713, 2025.

[46]. [41]. P. S. Ponnukumar, N. I. Francis Xavier, and R. Jaganathan, "Stable Plithogenic Cubic Sets," J. Fuzzy Ext. Appl., vol. 6, no. 2, pp. 410–423, 2025.

[47]. J. Ramkumar and V. Valarmathi, "Harnessing AI-Driven Models for Sustainable Development in Business Management," in World Sustainability Series, vol. Part F775, 2025, pp. 217–238.

[48]. S. P. Priyadharshini and J. Ramkumar, "Mappings Of Plithogenic Cubic Sets," Neutrosophic Sets Syst., vol. 79, pp. 669–685, 2025.

[49]. A. Senthilkumar, J. Ramkumar, M. Lingaraj, D. Jayaraj, and B. Sureshkumar, "Minimizing Energy Consumption in Vehicular Sensor Networks Using Relentless Particle Swarm Optimization Routing," Int. J. Comput. Networks Appl., vol. 10, no. 2, pp. 217–230, 2023.

[50]. J. Ramkumar, R. Karthikeyan, and K. O. Nitish, "Securing Library Data With Blockchain Advantage," in Enhancing Security and Regulations in Libraries with Blockchain Technology, 2024, pp. 117–138.

[51]. V. Valarmathi and J. Ramkumar, "Modernizing Wildfire Management Through Deep Learning and IoT in Fire Ecology," in Machine Learning and Internet of Things in Fire Ecology, 2024, pp. 203–229.

[52]. B. Suchitra, J. Ramkumar, and R. Karthikeyan, "Frog Leap Inspired Optimization-Based Extreme Learning Machine For Accurate Classification Of Latent Autoimmune Diabetes In Adults (LADA)," J. Theor. Appl. Inf. Technol., vol. 103, no. 2, pp. 472–494, 2025.

[53]. J. Ramkumar, V. Valarmathi, and R. Karthikeyan, "Optimizing Quality of Service

and Energy Efficiency in Hazardous Drone Ad-Hoc Networks (DANET) Using Kingfisher Routing Protocol (KRP)," Int. J. Eng. Trends Technol., vol. 73, no. 1, pp. 410–430, 2025.

[54]. R. Jaganathan, S. Rajagopal, and K. Rajendran, "Cultural Intelligence in the AI Era-Enhancing Transitional Higher Education," in Bridging Global Divides for Transnational Higher Education in the AI Era, 2024, pp. 273–292.

[55]. J. Ramkumar, A. Senthilkumar, M. Lingaraj, R. Karthikeyan, and L. Santhi, "Optimal Approach for Minimizing Delays in Iot-Based Quantum Wireless Sensor Networks Using Nm-Leach Routing Protocol," J. Theor. Appl. Inf. Technol., vol. 102, no. 3, pp. 1099–1111, 2024.

[56]. D. Jayaraj, J. Ramkumar, M. Lingaraj, and B. Sureshkumar, "AFSORP: Adaptive Fish Swarm Optimization-Based Routing Protocol for Mobility Enabled Wireless Sensor Network," Int. J. Comput. Networks Appl., vol. 10, no. 1, pp. 119–129, Jan. 2023.

[57]. J. Ramkumar, S. S. Dinakaran, M. Lingaraj, S. Boopalan, and B. Narasimhan, "IoT-Based Kalman Filtering and Particle Swarm Optimization for Detecting Skin Lesion," in Lecture Notes in Electrical Engineering, K. Murari, N. Prasad Padhy, and S. Kamalasadan, Eds., Singapore: Springer Nature Singapore, 2023, pp. 17–27.

[58]. J. Ramkumar, C. Kumuthini, B. Narasimhan, and S. Boopalan, "Energy Consumption Minimization in Cognitive Radio Mobile Ad-Hoc Networks using Enriched Ad-hoc On-demand Distance Vector Protocol," in 2022 International Conference on Advanced Computing Technologies and Applications, ICACTA 2022, Institute of Electrical and Electronics Engineers Inc., 2022.

[59]. P. Menakadevi and J. Ramkumar, "Robust Optimization Based Extreme Learning Machine for Sentiment Analysis in Big Data," in 2022 International Conference on Advanced Computing Technologies and Applications, ICACTA 2022, Institute of Electrical and Electronics Engineers Inc., 2022.

[60]. M. P. Swapna, J. Ramkumar, and R. Karthikeyan, "Energy-Aware Reliable Routing with Blockchain Security for Heterogeneous Wireless Sensor Networks," in Lecture Notes in Networks and Systems, V. Goar, M. Kuri, R. Kumar, and T. Senjyu, Eds., Springer Science and Business Media Deutschland GmbH, 2025, pp. 713–723.

[61]. J. Ramkumar and R. Vadivel, "Multi-Adaptive Routing Protocol for Internet of Things based Ad-hoc Networks," Wirel. Pers. Commun., vol. 120, no. 2, pp. 887–909, 2021.

[62]. R. Jaganathan and R. Vadivel, "Intelligent Fish Swarm Inspired Protocol (IFSIP) for Dynamic Ideal Routing in Cognitive Radio Ad-Hoc Networks," Int. J. Comput. Digit. Syst., vol. 10, no. 1, pp. 1063–1074, 2021.

[63]. R. Vadivel and J. Ramkumar, "QoS-enabled improved cuckoo search-inspired protocol (ICSIP) for IoT-based healthcare applications," Inc. Internet Things Healthc. Appl. Wearable Devices, pp. 109–121, 2019.

[64]. J. Ramkumar, R. Karthikeyan, and V. Valarmathi, "Alpine Swift Routing Protocol (ASRP) for Strategic Adaptive Connectivity Enhancement and Boosted Quality of Service in Drone Ad Hoc Network (DANET)," Int. J. Comput. Networks Appl., vol. 11, no. 5, pp. 726–748, 2024.

[65]. J. Ramkumar and R. Vadivel, "Whale optimization routing protocol for minimizing energy consumption in cognitive radio wireless sensor network," Int. J. Comput. Networks Appl., vol. 8, no. 4, pp. 455–464, 2021.

[66]. M. P. Swapna, D. Rajeev, J. Ramkumar, and S. Chandran, "Unveiling Cybercrime Patterns in Kerala: A Machine Learning Approach," in Lecture Notes in Networks and Systems, 2026, pp. 111–122.

[67]. R. Jaganathan, S. Mehta, and R. Krishan, "Preface," Bio-Inspired Intell. Smart Decis., pp. xix–xx, 2024.

[68]. R. Jaganathan, S. Mehta, and R. Krishan, "Preface," Intell. Decis. Mak. Through Bio-Inspired Optim., pp. xiii–xvi, 2024.